International Journal of Science and Research (IJSR)
ISSN (Online): 2319-7064
Index Copernicus Value (2015): 78.96 | Impact Factor (2015): 6.391

Development of Guar Gum based Magnetic Nanocomposite Hydrogels for the Removal of Toxic Pb^{2+} Ions from the Polluted Water

Alvakonda Narayanamma, Prof. K. Mohana Raju

Synthetic Polymer Laboratory, Department of Polymer Science & Technology

Sri Krishnadevaraya University, Anantapur-515055, Andhra Pradesh, India

Abstract: ***The present work highlights the development of guar gum containing magnetic nanoparticles and characterized for using heavy metal extraction. The magnetic nanoparticles (MNPs) were prepared in-situ in poly (acrylamide)-Guar gum P(GG-AM) hydrogels. The formation of magnetic nanoparticles in the hydrogel networks was determined by Fourier transform infrared spectroscopy (FTIR), Scanning electron (SEM) microscopy studies revealed the formation of MNPs throughout the hydrogel networks. The thermal properties of the hydrogel magnetic nanocomposites were confirmed by dynamic scanning calorimetry (DSC) and thermogravimetric (TGA) analysis.The magnetic properties of the synthesized hydrogel magnetic nanocomposites were determined by a vibrating sample magnetometer (VSM).The swelling properties of the hydrogel and the hydrogel magnetic nanocomposites investigated. The present works highlights the hydrogel magnetic nanocomposites used for the removal Pb(II). The results confirm that the hydrogel magnetic nanocomposites that exhibit superior extraction properties to hydrogels.***

Keywords: Magnetic Nanoparticles, Acrylamide (AM), Guar gum, Pb (II), Transmission electron microscopy (TEM), vibrating sample magnetometer

1. Introduction

Heavy metal pollution is a major environmental problem due to rapid global industrialization. Toxic heavy metals such as Cu, Co, Cr, Cd, Zn, and Zr are resistant to biological degradation and can accumulate in humans, causing health issues [28,65,66]. Waste water from textile industries contains a wide variety of toxic dyes which affect human health as well as photosynthetic process in aquatic biota [24].Pb is important in terms of protection of the public and environmental health as it attaches to proteins in the blood and conducted to different tissues in the body [43,44]. The elevated levels of Pb in surface waters originated from deposits of atmospheric dust, industrial waste water, urban runoff, and mine tailings [16].The control of Pb^{2+} pollution has special importance for both organisms that live in water and those that benefit from water [14].Traditional metal-removal techniques from water such as precipitation, oxidation, reduction, electrochemical treatment, reverse osmosis, solvent extraction, ion-exchange and evaporation are mostly expensive and difficult to apply [42].Biopolymers based adsorbents such as poly (methacrylic acid) grafted functionalized guar gum [55], cassia grandis seed gum-graft-poly (methyl methacrylate) [56] and 2-acrylamidoglycolic acid grafted xanthan gum [53]. Polymer nanocomposites are attractive over parental polymer, as they provide desirable porosity, large surface area, higher hydrodynamic radius, non-swelling nature, and excellent mechanical resistance [19,26,62] have been developed these polymers, having numerous functional groups such as carboxylic, amine, hydroxyl and sulfonic, could be used as complexing agents for the adsorptive removal of metal ions from aqueous solutions [21,13,8]. Polyacrylic acid (PAA) possesses many polar carboxylic groups form strong complexes with metal ions in solution [59].It has also been observed that polyacrylamide based water insoluble copolymers are efficient adsorbents for removal of heavy metals, such as polyacrylamide-grafted-coconut coir pith [4],cross linked polyacrylamide grafted guar gum [1], polyacrylamide grafted chitosan [38] etc.

Incorporation of magnetic nanoparticals provides additional functionalities for the binding of dye molecules [61].Composites containing single domain of magnetic nanoparticles within the hydrogel networks exhibit a unique phenomenon of superparamagnetism [39]. Biopolymers based magnetic nanocomposites have been successfully utilized previously for the decontamination of the organic dyes and metallic pollutants from waste water [5,50].Graft co-polymers Gg are used as superabsorbents for the recovery of crude oil in the petroleum industries [29], and as flocculants for the treatment of waste water [49]. The nanocomposite Guar gum based hydrogel shows excellent Pb^{2+} removal capacity (96.5%) from industrial wastewater. Magnetic nanoparticles (MNPs) have their potential applications in electronic, photonic, magnetic, and biomedical materials [9,31-33,36,63].Hydrogels synthesized by employing natural polymers and magnetic materials such as iron oxide (Fe_3O_4) or maghemite (γ-Fe_2O_3) have been widely used in many applications owing to their proven biocompatibility as well as quick response and sensitivity to external stimuli such as an applied magnetic field [7,35].Hydrogel–magnetic nanocomposites (HGMNCs) prepared by the employment of polysaccharide and magnetic nanoparticles [iron oxide (Fe_3O_4) or maghemite (c- Fe_2O_3)] have sensitivity to an external stimulus applied magnetic field[30,46].

Hydrogel water retention, network porosity, and elasticity properties enable them for vital applications such as

adsorbents for various metals [11], scaffolds [20], tissue engineering [54], bioseparation [34], drug delivery [25], and 3D composites [47]. Because of their porous nature hydrogels can offer suitable environments for the synthesis of various nanoparticles with enhanced stability.A number of hydrogel silver nanocomposites were evaluated for superior antimicrobial applications [40, 60]. Hydrogel magnetic nanocomposite materials offer the combined features of magnetic properties and conventional hydrogels [68].

Incorporation of MNPs into hydrogel networks results in hydrogel magnetic nanocomposites.This can result in superior interaction between the MNPs and the gel networks thereby improving their mechanical properties. If the ferrogels are constructed from MNPs of typical size of less than 20 nm they impart superparamagnetic properties [37].

Poly(acrylamide) hydrogels have been thoroughly studied as model hydrogel systems. PAM hydrogels are widely employed in purification, separation, and biomedical applications. To improve the swelling characteristics of PAM hydrogels additional natural polymers such as gum arabic or gum acacia (GA) are employed. The present investigation involves the synthesis and characterization of PAM-GA ferrogels incorporating MNPs of ca 10 nm size for metal extraction. In this scenario guar gum plays a vital role for MNP synthesis.

Guar gum is a naturally occurring galactomannan polysaccharide; consists of chiefly high molecular weight hydrocolloidal polysaccharide, composed of galactan and mannan units combined through glycosidic linkages and shows degradation in the large intestine due the presence of microbial enzymes. It contains about 80% galactomannan, 12% water, 5% protein, 2% acid soluble ash, and 0.7% fat. Guar gum has a molecular weight of approximately 1 million. A guar gum molecule is made up of about 10,000 residues, which are non-ionic polydisperse rod-shaped polymers (longer than found in locust bean gum)

The rate of guar gum dissolution and viscosity development generally increases with decreasing particle size, decreasing pH and increasing temperature. Hydration rates are reduced in the presence of dissolved salts and sucrose [6].Dilute solution of less than 1% concentration of guar gum are less thixotropic than solutions of concentration of 1% [23].Substitution of hydroxyl groups in guar gum with hydroxypropyl causes steric hindrance that decreases the stability of hydrogen bonds [15].Increase in concentration of guar gum enhances the inter-molecular chain interaction or entanglement which leads to increase in viscosity [64].On doubling the concentration guar gum shows tenfold increase in viscosity [10].Guar gum achieves its full viscosity in cold water unlike other gums,[18,22]. An increase in temperature causes the water molecules to lose their ordering around the guar gum molecule [57].It is non ionic and maintains a constant high viscosity over a broad range of ph. It was that reported the synthesis and characterization of novel guar gum hydrogels and their use as Cu(II) sorbent [12].The GGNPs used in cosmetics, biosensors, medical and food supplements. high viscosity guar gum derivatives can be obtained by treatment of guar gum with complexing agents like organic titanates, chromium salts and aluminum salts. Polyacrylamide is a water-soluble polymer with a hydrophobic main chain and hydrophilic functional groups in side chains.

Guar gum and its derivatives can be used for targeted drug delivery by forming coating matrix systems, hydrogels and nano-micro particles[48]. The sulfonated degraded guar gum also reported to reduce cholesterol and fibrinogen effectively [67]. It was found that the PHGG were found effective in treating cholera in adults [3].A hydrophilic polysaccharide matrix of guaran has been used for the preparation of some new chelating resins, after its cross linking with epoxychloropropane [2]. Guar gum based nanocomposite Gas sensor can be used for homeland security, gases leak detection in research lab and heavy metals removal from waste water. It is used in industries such as food, textile, pharmaceuticals, personal care, health Care, nutrition, cosmetics, paper, explosives, mining and oil well drilling. Guar gum mainly functions as a thickener, emulsifier, stabilizer, binding agent, gelling agent, Natural fiber, flocculant, fracturing agent etc. it is found to prevent the formation of ice crystals in ice-creams and aids in enhancing the freeze-thaw stability of solutions[58].Murthy et al. studied the applicability of carboxymethyl GG in transdermal drug delivery systems[41].The present work signifies the use of development of guar gum based magnetic nanocomposite hydrogels for the removal of toxic pb^{2+} ions from the polluted water.

2. Materials and Experimental Methods

The Preparation of Guar gum hydrogels with their code number and their feed compositions are presented in table 2.1.

Table 2.1: The details code numbers of biodegradable P(GG-AM) hydrogels and their feed compositions

S. No	*Sample Code*	*AM(g)*	*GG(g)*	*MBA ($\times 10^{-3}$ M)*	*KPS ($\times 10^{-3}$mM)*	*TMEDA ($\times 10^{-3}$ mM)*
1.	$P(GG\text{-}AM)_1$	1	0.05	1	1	1
2.	$P(GG\text{-}AM)_2$	1	0.1	1	1	1
3.	$P(GG\text{-}AM)_3$	1	0.15	1	1	1
4.	$P(GG\text{-}AM)_4$	1	0.2	1	1	1
5.	$P(GGM\text{-}AM)_1$	1	0.2	0.5	1	1
6.	$P(GGM\text{-}AM)_2$	1	0.2	0.75	1	1
7.	$P(GGM\text{-}AM)_3$	1	0.2	1.25	1	1
8.	$P(GGM\text{-}AM)_4$	1	0.2	1.5	1	1
9.	$P(GGK\text{-}AM)_1$	1	0.2	1	0.5	1
10.	$P(GGK\text{-}AM)_2$	1	0.2	1	0.75	1

11.	$P(GGK\text{-}AM)_3$	1	0.2	1	1.25	1
12.	$P(GGK\text{-}AM)_4$	1	0.2	1	1.5	1
13.	$P(GGT\text{-}AM)_1$	1	0.2	1	1	0.5
14.	$P(GGT\text{-}AM)_2$	1	0.2	1	1	0.75
15.	$P(GGT\text{-}AM)_3$	1	0.2	1	1	1.25
16.	$P(GGT\text{-}AM)_4$	1	0.2	1	1	1.5

3. Results and Discussion

3.1 Swelling properties

A successful adsorbent a material must have a large internal porosity with an adequate surface area for the adsorption process. Although nanoparticles have an enormous surface area for adsorption, poorer diffusion limits the adsorption rate and overall adsorption capacity. The combination of hydrogel networks and are an attractive potential solution in many potential applications. The HMNCs were developed in the present study by dispersing the colloidal MNPs (ca. 10 nm) throughout the P(GG-AM) hydrogels. GG is used in this study is due to its hydrophilicity, biocompatibility, biodegradability, and greater affinity for many bio macromolecules. GG can contribute to the stabilization of MNPs and extraction of metals and adsorption of proteins. A scheme of the synthetic approach followed to prepare the HMNC is shown in Scheme1.

A number of hydrogel formulations were prepared by free radical solution redox-polymerization of AM (1 g) by using different proportions of GG, cross-linker, initiator, and activator (step 1). The incorporation of iron salts into the hydrogels (step 2) and the precipitation of iron salts into Fe_3O_4 nanoparticles by the addition of ammonia results in HMNCs (step 3).The behavior of hydrogels, hydrogel composites, and hydrogel nanocomposites depends on the hydrogel network construction which determines its swelling capacity. In this study an optimized higher swelling capacity hydrogel was selected for the metal ion extraction. The same is shown in fig1. All the hydrogel compositions have shown ability to generate MNPs in the hydrogel networks resulting in HMNCs. GG polymer chains impart more hydrophilicity to the hydrogel networks resulting in improved swelling capacity. The overall order of the swelling capacity of these hydrogels was found to be Fe_3O_4 nanocomposite hydrogel > $Fe^{2+/}Fe^{3+}$ ions embedded hydrogel > P(GG-AM) hydrogel. When the hydrogels are treated with iron ions, the ions may be physically entrapped or chemically interact with hydroxyl anions of GG polymer or amide groups of PAM polymer chains, and disperse throughout the gel network. The electrostatic forces between the iron ions and amide/hydroxyl groups of hydrogels are responsible for the increase in the swelling capacity of hydrogels loaded with iron ions. The hydrogels loaded with iron ions were treated with ammonium hydroxide and MNPs form immediately and are stabilized inside the hydrogel networks. Their swelling capacity was observed for HMNCs compared to hydrogels loaded with iron ions and pure hydrogels. $P(GG\text{-}AM)_4$ hydrogel (0.2 g of GG, hereafter designated $P(GG\text{-}AM)_4$ and its iron ions/MNPs hydrogels have higher swelling capacity in P(GG-AM) series gels (Fig.1.1a).Owing to this, $P(GG\text{-}AM)_4$ was selected for further modification of gels on the basis of its higher swelling capacity in water. Increase of cross-linker concentration in the hydrogel synthesis leads to decreased swelling capacities of hydrogels owing to higher cross-linked networks (Fig.1.1b).Increasing of initiator/activator concentrations in the hydrogel synthesis slightly improved the swelling capacity of hydrogels (Fig.1.1c,d). No other hydrogel formulation exhibited greater swelling capacity than the $P(GG\text{-}AM)_4$ series hydrogels, i.e., $P(GG\text{-}AM)_4$, $P(GG\text{-}AM)_4$ hydrogel loaded with iron salts, and $P(GG\text{-}AM)_4$ magnetic nanocomposite. Therefore, all further studies were limited to only $P(GG\text{-}AM)_4$, $P(GG\text{-}AM)_4$, hydrogel loaded with iron salts, and $P(GG\text{-}AM)_4$ HMNC.

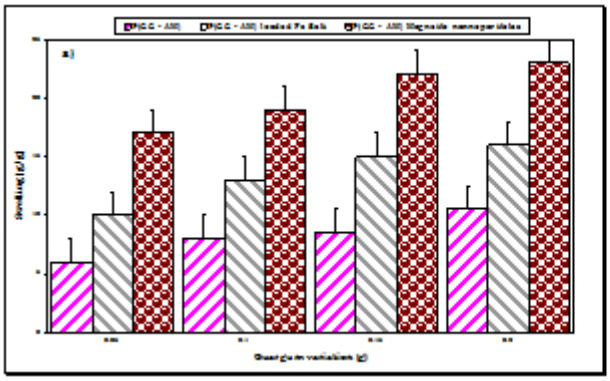

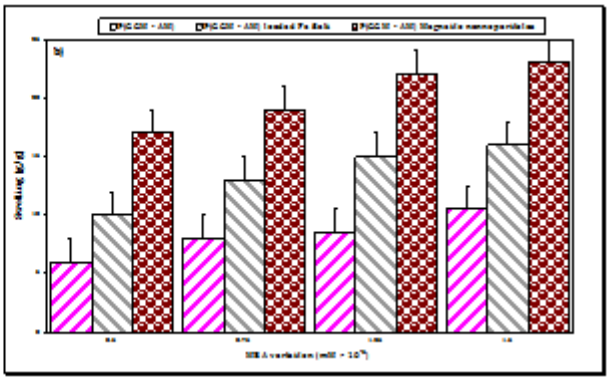

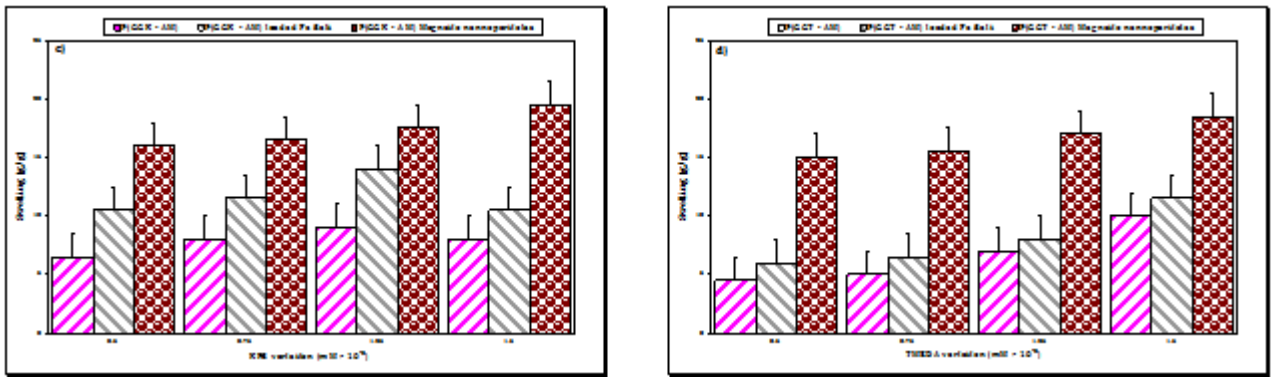

Figure 1.1. Swelling capacity of various hydrogels synthesized using different compositions of GG (a), MBA (b), KPS (c), and TMEDA (d), their subsequent hydrogels loaded with iron salts, and hydrogels containing Magnetic composites (HMNC).

3.2. Fourier transform infrared (FTIR) spectroscopy analysis

The developed P(GG-AM) and their iron (Fe_2O_3), magnetic nanocomposite hydrogels network were investigated by FTIR analysis. The Fig.1.2 shows the IR spectra of Pure GG, P(GG-AM),P(GG-AM) iron and P(GG-AM) magnetic nanocomposite hydrogels. The pure GG shows a broad absorption peak at 3345 cm^{-1} associated with the -OH symmetric stretching vibration and peaks at 1586cm^{-1} and 1496 cm^{-1} due to the aromatic ring quadrant stretching vibrations. The peaks at 1376 cm^{-1}, 1016 cm^{-1} and 996 cm^{-1} are associated with trihydroxybenzoate -C-O- stretching vibration of hydroxyl groups present in the aromatic ring of gallo moiety and –CH out of plane bending vibration was observed at 756 cm^{-1} due to the presence of 38.40% guar gum groups. The peaks are slightly moved in P(GG-AM) hydrogel. It is shown a broad absorption peaks at 3325.89 cm^{-1} that is related to the overlapping OH symmetric and NH asymmetric stretching vibrations groups and at 1576 cm^{-1} due to aromatic ring quadrant stretching due to the interaction of –OH group of the GG with –C=O group of the Am. All these peaks have further slightly shifted to 3235 cm^{-1} and ,1606,1576 cm^{-1} in Fe_3O_4, magnetic nanocomposite hydrogel and a new sharp peak was absorbed at 767 cm^{-1}due to the stretching vibrations of the Fe-O of Fe_3O_4 and magnetic confirming the presence of iron oxide, magnetic, nanoparticles in the hydrogel matrix. By this it can be concluded that Fe_3O_4, magnetic nano particles are present in P(GG-AM) hydrogels.

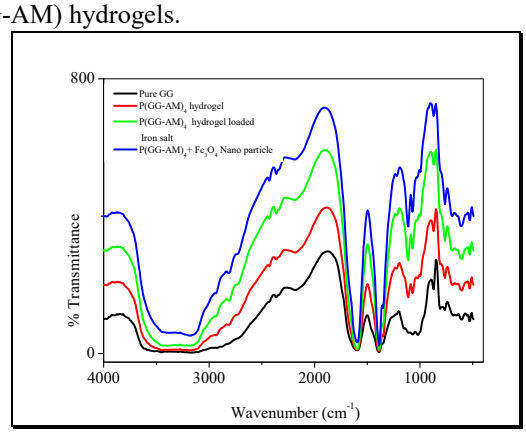

Figure 1.2: FTIR spectra of pure GG, $P(GG\text{-}AM)_4$ hydrogel, $P(GG\text{-}AM)_4$ hydrogel loaded with iron salts P $(GG\text{-}AM)_4$+Fe_3O_4 nanocomposite hydrogel

3.3 Thermal studies

The thermal stability and the formation of the hydrogels and their Fe_3O_4 nanocomposites were analysed with DSC and TGA analysis.

3.3 (a) Differential scanning calorimetry (DSC)

Fig.1.3. shows the DSC curves of pure GG, $P(GG\text{-}AM)_4$ hydrogel, $P(GG\text{-}AM)_4$ hydrogel loaded iron salt and Fe_3O_4 nanocomposite hydrogel, obtained by testing in nitrogen atmosphere at a heating rate of 10^0C/min. $P(GG\text{-}AM)_4$ hydrogel showes a peak at 240^0C due to the formation of hydrogel and Fe_3O_4 nano particles embedded hydrogel displays a stronger peak at 255^0C when compared to $P(GG\text{-}AM)_4$ hydrogel in DSC (Fig1.3) studies. This is due to the incorporation of Fe_3O_4 nano particles in the hydrogel network. A common small endothermic peak was absorbed at 89.28^0C in all the three cases that is Pure GG, $P(GG\text{-}AM)_4$ hydrogel and Fe_3O_4 nanocomposite hydrogel due to the presence of moisture in the samples.

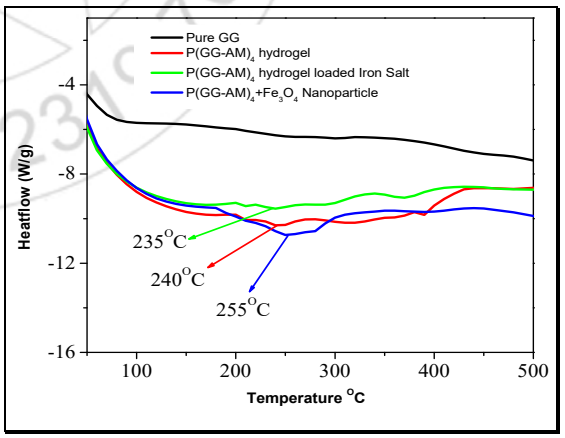

Figure 1.3: DSC thermograms of pure GG, $P(GG\text{-}AM)_4$ hydrogel, $P(GG\text{-}AM)_4$ hydrogel loaded with iron salts, and $P(GG\text{-}AM)_4$+Fe_3O_4 nanocomposite hydrogel

3.3 (b) Thermogravimetric analysis (TGA)

The percentage weight loss of pure GG, $P(GG\text{-}AM)_4$, $P(GG\text{-}AM)_4$+Fe_3O_4,and $P(GG\text{-}AM)_4$+Fe_3O_4, nanocomposite hydrogel was characterized by thermogravimetric analysis to determine the weight loss at certain temperature. Fig 1.4 shows the percentage decomposition of hydrogel and their

Fe_3O_4 nanocomposite hydrogel. From the TGA thermogram, the weight loss observed in the case of P (GG-AM)$_4$ hydrogel is 18.83% at 600^{O}C (Fig 1.4), whereas the weight loss in Fe_3O_4 nanocomposite hydrogel is (36.52%) at this temperature (600^{0}C) (Fig 1.4).The difference in decomposition between the hydrogel and Fe_3O_4 nanocomposite hydrogel is found to be 17.69% and it confirms the presence of Fe_3O_4 nanoparticles (weight loss) in the hydrogel network.

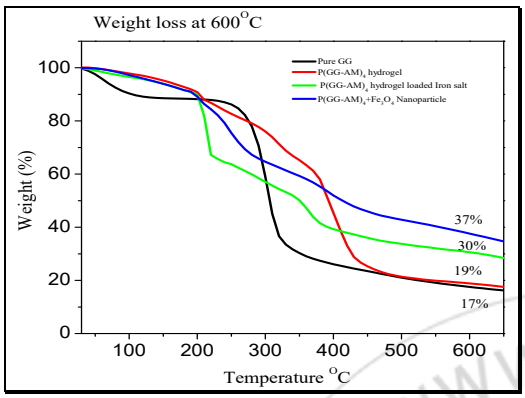

Figure 1.4: TGA curves of pure GG, P(GG-AM)4 hydrogel, P(GG-AM)$_4$ hydrogel loaded with iron salts, and P(GG-AM)$_4$+Fe_3O_4 nanocomposite hydrogel

3.4 Scanning electron microscopy (SEM)

The surface morphology of P(GG-AM)$_4$ and Fe_3O_4 nanocomposite hydrogels were investigated with SEM. Fig.1.5(A-C) shows the SEM micrographs of the P(GG-AM)$_4$ and Fe_3O_4 nanocomposite hydrogels. Fig. 1.5(A) shows a clearly rough surface morphology for P(GG-AM)$_4$ hydrogel, whereas Fe_3O_4 nano particles embedded hydrogel exhibited smaller nanoparticles dispersed throughout the gel network Fig. 1.5(B) and Fig.1.5(C) shows with different magnifications. It was found that no individual Fe_3O_4 nano particles were observed outside the P(GG-AM)$_4$ hydrogels, indicating a strong interaction between the P(GG-AM)$_4$ and the Fe_3O_4 particles confirming the presence of Fe_3O_4 nano particles within the P(GG-AM)$_4$ hydrogel.

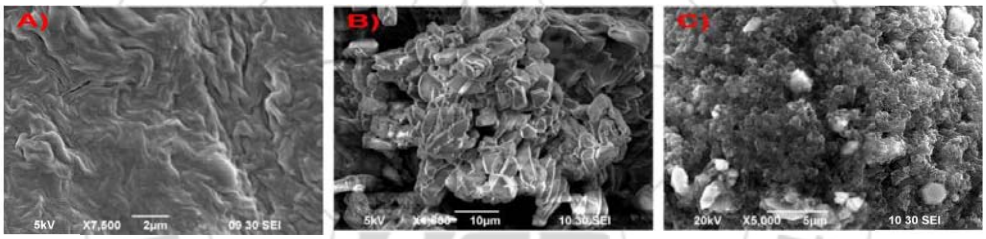

Figure 6.5: SEM images of : (A) P(GG-AM)$_4$ hydrogel,(B) P(GG-AM)$_4$ hydrogel loaded with iron salts (C) P(GT-AM)$_4$+ Fe_3O_4 nanocomposite hydrogel

3.5 X-ray diffraction (XRD) analysis

To study the crystallographic nature of Iron oxide nano particles and the nanocomposite the XRD analysis was performed and the corresponding XRDs are shown in (Figure 1.6) P(GG-AM)$_4$ and P(GG-AM)$_4$ hydrogel loaded iron salts have not exhibited any sharp peaks in XRD. A broad peak at 250 is due to the polymer network. Figure 6.6 shows the X-ray diffraction pattern of the Fe_3O_4 nanocomposite P(GG-AM)$_4$ hydrogel and the insert spectra shows for pure GG, P(GG-AM)$_4$ hydrogel. The Fe_3O_4 nanocomposite hydrogel shows the diffraction peaks at about 29.9 (111), 35.03 (311), 42.08 (400), 57.20 (511), and 63.52 (440) (Figure 6.6), Figure 1.6(A) shows that standard Fe_3O_4 crystal diffraction peaks which is coincident to the data of cubic Fe_3O_4.The common diffraction peak has been observed at 2θ=23.45 and 42.3^{0}C in pure GG, P(GG-AM)$_4$ and Fe_3O_4 nanocomposite hydrogels showing the amorphous nature of the pure GG and P(GG-AM)$_4$ hydrogel.The well defined X-ray diffraction patterns indicate the formation of highly crystalline iron oxide nano particles. These results indicate that the prepared nanoparticles are pure magnetite with an inverse cubic spinal structure, which are identical to the standard XRD patterns of Fe_3O_4.

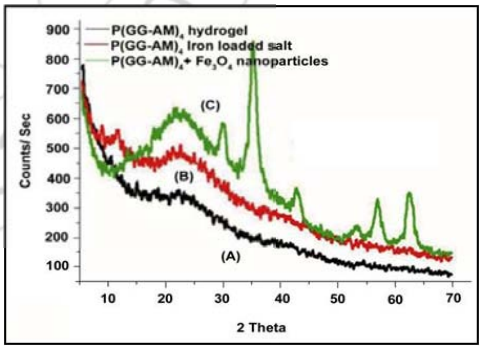

Figure 1.6: XRD patterns of P(GG-AM)$_4$ hydrogel, P(GG-AM)$_4$ hydrogel loaded with iron salts and P(GG-AM)$_4$ +Fe_3O_4 nanocomposite hydrogel

3.6 Transmission Electron Microscope (TEM) Analysis

Fe_3O_4 nano particles size is determined by using the TEM analysis and the analysis indicates the formation of spherical Fe_3O_4 nano particles in P(GG-AM)$_4$ hydrogel network. The Fe_3O_4 nano particles TEM image is shown in Fig.1.7. The average size of the particles is about $\sim 10\,nm$. This is due to the strong interaction between the Fe_3O_4 nano particles and P(GG-AM)$_4$ hydrogel network and Fe_3O_4nano particles are stabilised by using GG in the hydrogel network.

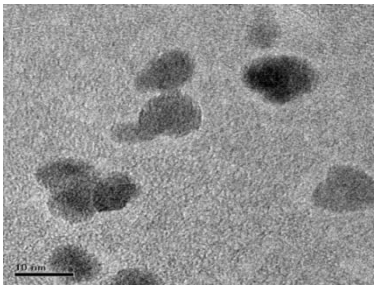

Figure 1.7: TEM images of Fe_3O_4 nanoparticles of P(GG-AM)$_4$ hydrogel

3.7 Magnetization studies using Vibrating Sampling Magnetometer (VSM) Analysis

Magnetic properties of a nanocomposite material are of great significance as their magnitude ultimately determines the nature of the applications [27].To explore the nature of the prepared nanocomposites' magnetic behavior, we investigated the variation in their magnetic moments as a function of the magnetic field in the range of −15,000 to 15,000 Oe. The results are shown in Fig. 1.8 which represents the magnetization–coercivity plots for P (GG-AM)$_4$ and P(GG-AM)$_4$+Fe_3O_4 nano particles. The saturation magnetization (Ms) and coercivity (Hc) of the P(GG-AM)$_4$+Fe_3O_4 nano particle were found to be 7.5 emu/g and 14,731 Oe orderly.This magnetization value is far below that of pure magnetic nano particles (Fe_3O_4) (66.1 emu/ g) it is due to because of the presence of only ca. 15.5% of MNPs in the hydrogel (theoretical Ms 9.254 emu/g, experimental 7.5 emu/g).A single domain of magnetic nano particles formed within the hydrogel networks exhibits the unique phenomenon of superparamagnetism [17].

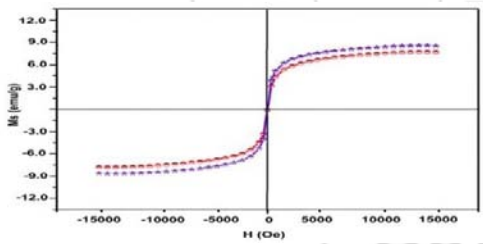

Figure 1.8: Magnetization saturation curves of P (GG-AM)$_4$ HMNC (violet curve) and P(GG-AM)$_2$ HMNC (red curve)

3.8 Metal absorption studies

Waste water from many industries, such as tanning, chemical manufacturing, mining, and battery manufacturing contains toxic heavy metals. Such metals are not biodegradable and tend to accumulate in living organisms, causing various diseases and disorders. Led is listed among 11 pollutants designated hazardous priority substances [51]. Recently absorbents with magnetic properties have gained much attention due to their ability to readily absorb and remove pollutants from aqueous environments on application of a magnetic field [45,52].This study reveals that the developed HMNC is a versatile material to remove various toxic metal ions from aqueous environments.

For the absorption studies P(GG-AM)$_4$ hydrogel, P(GG-AM)$_4$+ Fe_3O_4 hydrogel nano composite (HMNC), and P(GG-AM)$_4$ hydrogel loaded iron salt were utilized. Crushed hydrogel powder ($200\ \mu m$) was mixed in 0.5 M Pb(II) metal ion solutions. At different intervals the metal ion concentrations were determined by UV–Vis spectrophotometry. It can be seen clearly in (Fig. 1.9a) that P (GG-AM)$_4$+ Fe_3O_4 hydrogel nano composite, (HMNC) demonstrated an excellent absorption capacity by lowering the metal ion concentration in the solution (24 h reading). The investigated order of absorption capacity of metal ions is HMNC (P(GG-AM)$_4$) > P(GG-AM)$_4$+Fe_3O_4 > P(GG-AM)$_4$. At time points similar absorption behavior occurred (Fig. 1.9). The overall metal and protein adsorption capacities of these HMNCs are presented in Table.

Table 1.2: Metal adsorption capacities of different Guar Gum concentrations.

Sample	*Amount of Fe_3O_4 (%)[a]*	*Amount of metal absorbed at equilibrium (mg/g)*
Blank hydrogel	-	140.5387
GG_4 hydrogel	-	120.2563
GG_1 HMNC (0.1g of GG)	7.5	*132.5236*
GG_2 HMNC (0.2g of GG)	*9.04*	141.8596
GG_3 HMNC (0.3g of GG)	12.05	155.2698
GG_4HMNC (0.4g of GG)	13.92	178.5231

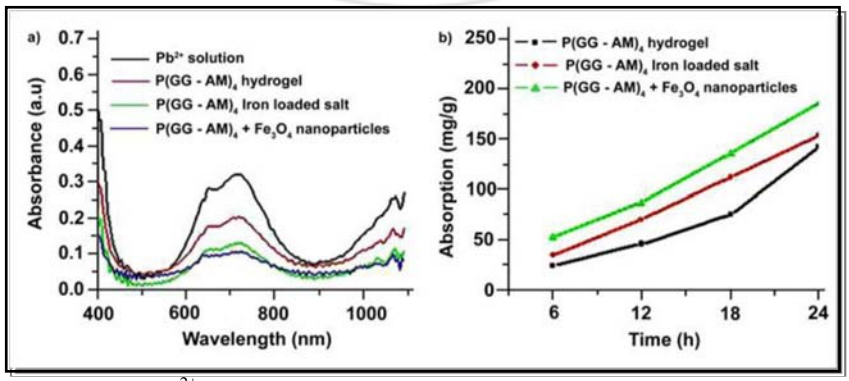

Figure 1.9 : (a) UV-Vis spectra of Pb^{2+} solutions at 24h after treating with P(GG-AM)$_4$ hydrogel, P(GG-AM)$_4$ iron loaded salt, P(GG-AM)$_4$+Fe_3O_4 nanocomposite. (b) Absorption capacity of various hydrogels at different time intervals

4. Conclusions

The prepared gels were characterized by FTIR spectroscopy, X-ray diffraction, and thermal studies (TGA). In the present investigation it was found that GG polymer chains impart more hydrophilicity to the hydrogel networks resulting in improved swelling capacity.The magnetic properties of the developed hydrogel magnetic nanocomposites were conformed. The formation of Fe_3O_4 nanoparticles within the hydrogel network structure was confirmed by using SEM and the particles average size was about ~ 10nm.

The increase of GG and MBA amount in the hydrogels increases the swelling of the hydrogel and formation of more amount of Fe_3O_4 nano particles as evidenced by swelling analysis. The drug releasing profiles of the magnetic hydrogel samples were also studied under external magnetic field. Overall the use of GG in the hydrogel networks enhances the swelling capacity of the hydrogels and colloidal stability of the Fe_3O_4 nano particles. In conclusion the prepared polymer matrices have exhibited both superparamagnetic and biocompatible properties are useful as potential candidates for biomedical applications.

References

[1] Abdel-Halim, E.S., Al-Deyab, S.S.,Hydrogel from crosslinked polyacrylamide/ guar gum graft copolymer for sorption of hexavalent chromium ion. Carbohydr. Polym. 86, (2011) ,1306–1312.
[2] Ahuja M and Rai AK ,Adsorption studies with some chelating ion exchange resins derived from guaran. Carb. Polym. 33 (1), (1997), 57-62.
[3] Alam NH, Ashraf H, Sarker SA, Olesen M, Troup J, Salam MA, Gyr N and Meier R. Efficacy of partially hydrolyzed guar gum-added oral rehydration solution in the treatment of severe cholera in adults. 78(1), Digestion (2008), 24-9.
[4] Anirudhan, T.S., Unnithan, M.R., Divya, L., Senan, P,Synthesis and characterization of polyacrylamide grafted coconut coir pith having carboxylate functional group and adsorption ability for heavy metal ions. J. Appl. Polym. Sci. 104,(2007), 3670–3681.
[5] Banerjee, S. S., & Chen, D. H, Fast removal of copper ions by gum Arabic modified magnetic nano-adsorbent. Journal of Hazardous Materials, 147, (2007),792–799.
[6] Bemiller JN, Whistler RL Industrial gums: polysaccharides and their derivatives. Academic Press, (1993).
[7] Bhattarai SR, Bahadur KCR, Aryal S, Khil MS, Kim HY Carbohydr Polym (2007) ,69:467.
[8] Bleiman N, Mishael YG ,Selenium removal from drinking water by adsorption to chitosan–clay composites and oxides: batch and columns tests. J Hazard Mater 183:5(2010),90–595.
[9] Burda C, Chen XB, Narayana R, Sayed EI Chemi Revie 105, (2005),1025.
[10] Carlson WA, Ziegenfuss EM, Overton JD,Compatibility and manipulation of guar gum. Food Technol 16: (1962),50–54.
[11] Chauhan GS, Chauhan S, Sen U, Garg D Desalination 243, (2009) ,95.
[12] Chauhan K, Chauhan GS and AHN JH ,Synthesis and characterization of novel guar gum hydrogels and their use as Cu (II) sorbent. *Biosour. Technol*. **100** (3), (2009) , 3599-3603.
[13] Chen H, Wang A,Adsorption characteristics of Cu(II) from aqueous solution onto poly(acrylamide)/attapulgite composite. J Hazard Mater 165: (2009) ,223–231.
[14] Chen, H., Wang, A., Kinetic and isothermal studies of lead ion adsorption onto palygorskite clay. J. Colloid Interface Sci. 307,(2007), 309–316.
[15] Cheng Y, Prud'homme RK,Measurement of forces between galactomannan polymer chains: effect of hydrogen bonding. Macromolecules 35:(2002), 10155–10161.
[16] Chern EC, Tsai DW, Ogunseitan OA,Deposition of glomalinrelated soil proteins and sequestered toxic metals into watersheds. Environ Sci Technol 42: (2007),3566–3572.
[17] Chia CH, Zakaria S, Ahamad S, Abdullah M, Jani SM,Am J App Sci 3:1750, (2006) ,1546–9239.
[18] Chudzikowski RJ. Guar gum and its applications. Journal of the society of cosmetic chemistry,22: (1971), 43-60.
[19] Darder, M., Ruiz-Hitzky, E., Caramel–clay nanocomposites. J. Mater. Chem. 15, (2005), 3913–3918.
[20] Drury JL, Mooney DY,Biomaterials 24: (2003), 4337.
[21] Futalan CM, Kan C, Dalida ML, Hsien K, Pascua C, Wan M ,Comparative and competitive adsorption of copper, lead, and nickel using chitosan immobilized on bentonite. Carbohydr Polym 83: (2011),528–536.
[22] Gittings MR, Cipelletti L, Trappe V, Weitz DA, In M and Lal J. The effect of solvent and ions on the structure and rheological properties of Guar solutions. Journal of Physical Chemistry, 105: (2001),9310-9315.
[23] Glicksman M,Gum technology in the Food Industry Academic Press; New York (1969).
[24] Goncalves, I. M., Ferra, M. I., & Amorim, M. T. P,Processos de remocao biologica de corantes nos efluentes de industria textile. Tecnologias do Ambiente, 11,(1996),35–38.
[25] Gupta P, Vermani K, Garg S ,Drug Discov Today 7:5(2002),69.
[26] Huang, Z.H., Zheng, X., Lv, W., Wang, M., Yang, Q.H., Kang, F., Adsorption of lead(II) ions from aqueous solution on low-temperature exfoliated grapheme nanosheets. Langmuir 27, (2011),7558–7562.
[27] Jain TK, Morales MA, Sahoo SK, Leslie-Pelecky DL, Labhasetwar V Mol Pharam 2: (2005),194.
[28] Jang SH, Jeonga GY, Mina BG, Lyoob WS, Lee SC ,J Hazard Mater 159,(2008),294.
[29] Kaith, B. S., Jindal, R., Mittal, H., & Kumar, K, Synthesis, characterization and swelling behavior evaluation of Gum ghatti and acrylamide based hydrogel for selective absorption of saline from different petroleum fraction-saline emulsions. Journal of Applied Polymer Science, 124, (2012),2037–2047.
[30] Kato, N.; Takizawa, Y.; Takahashi, F. J. J. Intell Mater Sys Struct 8, (1997),588.
[31] Kim BJ, Bang J, Hawker ET, Krammer EJ,Macromolecules 39: (2006),4108.

[32] Kim DH, Kim SH, Lavery K, Russell TP,Nano Lett 4: (2004),1841.
[33] Kim HC, Jia XO, Stafford CM, Kim DH, Mccarthy TJ, Tuominen M Adv Mater 13: (2001),795.
[34] Kim JJ, Park K,Bioseparation 7: (1998),177.
[35] Lao LL, Ramanujan RV,J Mater Sci Mater Med 15: (2004),1061.
[36] Lazzari M, Quintela MAL ,Adv Mater 159: (2003),1583.
[37] Li B, Jia D, Zhou Y, Hu Q, Cai W,J Magn Magn Mater 306: (2006) 223.
[38] Li, N., Bai, R., Liu, C.,Enhanced and selective adsorption of mercury ions on Chitosan beads grafted with polyacrylamide via surface-initiated atom transfer radical polymerization. Langmuir 21, (2005),11780–11787.
[39] Liu.S. L. Zhang, J. Zhou, J. Xiang, J. Sun, J. Guan, Fiber like Fe_2O_3 macroporous nanomaterials fabricated by calcinating regenerate cellulose composite fibers, Chem. Mater. 20 (2008), 3623–3628
[40] Murthy PSK, Mohan YM, Varaprasad K, Sredhar B, Mohana Raju K,J Colloid Interface Sci 318: (2008),217.
[41] Murthy S N,HiremathS.R.R.,Paranjothy K.L.K., Int. J. Pharm,272 (2004),11–18.
[42] O¨zcan AS, Go¨k O, O¨ zcan A,Adsorption of lead(II) ions onto 8-hydroxy quinoline-immobilized bentonite. J Hazard Mater 161: (2009),499–509.
[43] Ogunseitan OA,Public health and environmental benefits of adopting lead-free solders. JOM 59: (2007) ,12–17.
[44] Ogunseitan OA, Yang S, Ericson JE,Microbial delta-aminolevulinate dehydratase as a biosensor of lead (Pb) bioavailability in contaminated environments. Soil Biol Biochem 32: (2000),1899–1906.
[45] Ozay O, Kici SE, Baran Y, Aktas N, Sahiner N,Water Res 43: (2009),4403.
[46] Panevo, D.; Stoilova, O.; Manolova, N.; Rashkov, I. E-Polymer, 60,(2004),1.
[47] Polizzotti BD, Fairbanks BD, Anseth KS,Biomacromolecules 9: (2008),1084.
[48] Prabhaharan M. Prospective of Guar gum and its derivatives as controlled drug delivery system. International Journal of Biological Macromolecules 49(2):(12011),17-124.
[49] Rani, P., Sen, G., Mishra, S., & Jha, U.Microwave assisted synthesis of polyacrylamide grafted gum ghatti and its application as flocculant. Carbohydrate Polymers, 89, (2012),275–281.
[50] Rocher, V., Siaugue, J. M., Cabuil, V., & Bee, A, Removal of organic dyes by magnetic alginate beads. Water Research, 42, (2008),1290–1298.
[51] Rozada F, Otero M, Moran A, Garcia AI,Bioresour Technol 99: (2008),6332.
[52] Sahiner N, Ozay O React Funct Polym 71:6(2011),07.
[53] Sand, A., Yadav, M., & Behari, K,Graft co-polymerization of 2- acrylamidoglycolic acid onto xanthan gum and study of its physicochemical properties. Carbohydrate Polymers, 81,(2010),626–632
[54] Shu XZ, Liu Y, Palumbo FS, Luo Y, Prestwich GD (2004) Biomaterials 25:1339.
[55] Singh, V., Kumari, P., Pandey, S., & Narayan, T,Removal of chromium (VI) using poly(methylacrylate) functionalized guar gum. Bioresource Technology, 100, (2009),1977–1982.
[56] Singh, V., Tiwari, S., Sharma, A. K., & Sanghi, R, Removal of lead from aqueous solutions using Cassia grandis seed gum-graft-poly(methylmethacrylate). Journal of Colloid and Interface Science, 316, (2007),224–232.
[57] Srichamroen A. Influence of temperature and salt on the viscosity property of Guar gum. Naresuan University Journal 15(2): (2007),55-62.
[58] Surendra, T Das, M.K. Guar Gum Present Status and Applications, Journal of Pharmaceutical and Scientific Innovation; 4 July – August (2013), 24 – 28.
[59] Tran NH, Dennis GR, Milev AS, Kannangara GSK, Wilson MA, Lamb RN Interactions of sodium montmorillonite with poly(acrylic acid). J Colloid Interface Sci 290: (2005), 392–396
[60] Vimala K, Sivudu KS, Mohan YM, Sreedhar B, Mohana Raju K Carbohydr Polym 75: (2009),463.
[61] Xu, Y. Y., Zhou, M., Geng, H. J., Hao, J. J., Ou, Q. Q., Qi, S. D., et al,A simplified method for synthesis of Fe_3O_4@PAA nanoparticles and its application for the removal of basic dyes. Applied Surface Science, 258, (2012),3897–3902.
[62] Yang, S., Hu, J., Chen, C., Shao, D., Wang, X,Mutual effects of Pb(II) and humic acid adsorption on multiwalled carbon nanotubes/Polyacrylamide composites from aqueous solutions. Environ. Sci. Technol. 45,(2011),3621–3627.
[63] Yeh SW, Wu TL, Wei KH Nanotechnology 16:(2005) 683. doi:10.1088/0957-4484/16/6/010
[64] Zhang LM, Zhou JF, Hui PS,A comparative study on viscosity behavior of water-soluble chemically modified guar gum derivatives with different functional lateral groups. J Sci Food Agric 85: (2005),2638– 2644
[65] Zhou L, Wang Y, Liu Z, Haung Q,J Hazard Mater 161: (2009),995. doi:10.1016/j.jhazmat.2008.04.078
[66] Zhou YT, Nie HL, White GB, He ZY, Zhu LM ,J Colloid Interface Sci 330: (2009),29. doi:10.1016/j.jcis.2008.10.026
[67] Zhu Y, Fang B, Huang L, Guan C and Yang G. Study on the selective removal of plasma low-density lipoprotein and fibrinogen by degraded guar sulfate. Sheng Wu, Yi Xue, Gong Cheng, Xue Za Zhi 25(5): (2008),1135-40.
[68] Zrínyi M, Barsi L, Büki A,Polym Gels Netw 5:(1997),415. doi:10.1016/S0966-7822(97)00010-5